Available online at www.sciencedirect.com
ScienceDirect
Thin Solid Films 516 (2008) 8146–8149
www.elsevier.com/locate/tsf

Effect of chlorine doping on electrical and optical properties of ZnO thin films

E. Chikoidze [a,*], M. Nolan [b], M. Modreanu [b], V. Sallet [a], P. Galtier [a]

[a] Groupe d'Etude de la Matière Condensée (GEMaC), CNRS, Université de Versailles-Saint-Quentin, 1 Place Aristide Briand. 92195 Meudon Cedex, France
[b] Tyndall National Institute, University College Cork, Lee Maltings, Prospect Row, Cork, Ireland

Available online 18 April 2008

Abstract

Chlorine doped ZnO thin films were grown by metal-organic chemical vapour deposition (MOCVD) on sapphire and fused silica substrates. Chlorine is incorporated by substitution of oxygen and acts as a donor, leading to an increase of electron concentration. Transport properties were studied for ZnO thin films with different chlorine content. Hall effect measurements show an increase of electron carrier concentration and a decrease of electron mobility upon increasing the amount of chlorine incorporated in ZnO. The lowest resistivity $\rho = 3.6 \times 10^{-3}$ Ω cm was obtained for layers deposited on sapphire substrate. UV–VIS–NIR spectroscopy has been used for the study of optical properties. For all samples, the optical transmittance in the visible range is greater than 80%. First principles computations were applied in order to examine the change in the band gap of ZnO with Cl doping.

Keywords: ZnO; 15.Gh; 73.61s.; 78.30.Fs; 78.40; 78.60.Hk

1. Introduction

ZnO is a well known intrinsic, n-type semiconductor [1,2] and has a broad range of applications in optoelectronics, acoustic devices and light-emitting diodes. As a semiconducting oxide material with low resistivity, high transmittance down to the UV spectral range, and good chemical stability under strong reducing environments, ZnO is thus a promising transparent conductive oxide (TCO) and a possible alternative to tin oxide and indium oxide to be used as transparent electrode for photovoltaic solar cells and electrodes on flat panel displays [3]. Up to now, metal elements like Al [4,5], Ga [6,7], Ba [8], Sc [8], Cu [9], Fe [9], Sn [9] and In [9,10], which substitute for Zn, have been widely used for this purpose. There are a few studies [11–13] where fluorine substitutes for oxygen. To our knowledge, with the exception of one report [14], there are no data in the literature for chlorine doping of ZnO. In this paper we investigate the effect of chlorine doping on electrical and optical properties of ZnO using experiment and first principles computations.

2. Experimental details

ZnO and ZnO:Cl layers have been grown by metal-organic chemical vapour deposition (MOCVD) in a vertical geometry reactor. Diethyl-zinc (DEZ), *n*-Butyl Chloride (*n*-BuCl), ($CH_3(CH_2)_3Cl$) and tertiary-butanol (*t*-Bu) have been used as zinc, chlorine and oxygen sources, respectively. The chlorine precursor is a liquid (melting point −123 °C) and was used at different temperatures from 0 °C to 20 °C. The carrier gas was H_2 with a 0.12 m^3/h flow. The growth was performed on two types of substrates: (001) oriented sapphire pre-treated in oxygen atmosphere at 1100 °C for 8 h and synthetic fused silica. In all cases the growth temperature was $T = 425$ °C. For most of the results reported in this paper, the DEZ pressure, P(DEZ), was fixed to 30.3 Pa, the pressure of *t*-Bu ranged from 30 to 160 Pa, while the pressure for *n*-BuCl was varied between 3.8 and 250 Pa. (The indicated values of pressures are the partial pressures of the gases in the reactor). When the pressures of zinc and chlorine precursors are fixed, the growth rate increases with increasing the pressure of *t*-Bu. No significant change of growth rate has been observed with chlorine incorporation, using either silica or sapphire substrates. Growth rate was about 1.4 μm/h in the case of silica substrate and 2.5 μm/h for sapphire. The purity

* Corresponding author. Tel.: +33 145075285; fax: +33 145 07 58 41.
E-mail address: Ekaterina.chikoidze@cnrs-bellevue.fr (E. Chikoidze).

0040-6090/$ - see front matter © 2008 Elsevier B.V. All rights reserved.
doi:10.1016/j.tsf.2008.04.076

of the phase was checked by standard θ–2θ X-ray diffraction scans with Cu–Kα wavelength. The crystal orientation and quality of the films deposited on *c*-sapphire were investigated by high resolution X-ray diffraction (XRD) with 20″ resolution. The thickness of the samples grown on fused silica was 0.7 μm and was measured by optical interferences using a Nanocalc 2000, whereas the thickness of layers grown on sapphire substrates, ranging from 1 μm to 1.5 μm, as determined by depth profilometry associated to secondary ion mass spectrometry (SIMS). The chlorine concentration in the samples was determined by SIMS. Carrier concentration and mobility were measured by standard resistivity and Hall effect set-ups in the Van der Pauw configuration with indium metal as the electrical contacts. A double beam spectrophotometer (Perkin Elmer Lambda 950) equipped with an integrated sphere was used for the UV–VIS–NIR transmission measurements.

3. Results and discussion

3.1. Structural and electrical properties

The structural properties of chlorine doped ZnO films were studied by X-ray diffraction (XRD). Films grown on sapphire substrate are epitaxially grown, the full width at half maximum (FWHM) of the Ω-scan of the (002) peak in the case of pure ZnO grown on sapphire is 0.29°, while after incorporation of chlorine, the FWHM became larger, around 0.43°. For all ZnO:Cl samples grown on silica independently of doping level, the pure wurtzite structure is maintained. The films are highly textured with preferential orientation along the *c* axis.

Transport properties were studied at room temperature. Pure ZnO grown on sapphire with DEZ=30 Pa and *t*-Bu=161 Pa vapour pressure exhibited a resistivity of $\rho=1.8\times10^{-1}$ Ω cm and a mobility of $\mu=35$ V^{-1} s^{-1} cm^2 and an electron concentration of $n=10^{18}$ cm^{-3}. Keeping the same pressures for DEZ and *t*-Bu ($P_{t\text{-Bu}}/P_{\text{DEZ}}=5.3$), and increasing the chlorine vapour pressure from 3.8 to 104 Pa, for the layers grown on sapphire, lead to an increase of carrier concentrations, reaching a maximal value of 1.77×10^{20} cm^{-3}. From SIMS measurements we have determined a 0.02%(N(Cl)=1.2×10^{19} cm^{-3}) doping level of Cl for ZnO:Cl samples grown with P(*n*-BuCl)=31 Pa and a maximum doping level of 0.5% Cl (N(Cl)=4×10^{20} cm^{-3}) in the case of (P(*n*-Bu)=84 Pa). The electron concentration also increases with chlorine vapour pressure for the silica substrate. When the chlorine pressure exceeds 104 Pa the concentration of free carriers starts to decrease. It seems that for these growth conditions, we reach the solubility limit of Cl in the ZnO matrix and this element does not substitute oxygen anymore, but creates some kind of compensating centers. Other group III elements (Al, In, Ga) show quite a high solubility, up to 7% [7,15,16]. The low solubility of chlorine is probably related to the large ionic radius of chlorine compared to Zn.

Mobilities for all ZnO:Cl samples grown on sapphire and silica substrates decrease with an increase of chlorine content in the layers. When P(*n*-BuCl) <100 Pa, the mobility decreases more significantly from 35 V^{-1} s^{-1} cm^2 (pure ZnO) to 14 V^{-1} s^{-1} cm^2 and for P (*n*-BuCl) >100 Pa, there is a comparatively small (9–12 V^{-1} s^{-1} cm^2) variation of mobility. At room temperature, the mobility in the films with low carrier concentrations is influenced mostly by the scattering of free carriers off phonons, while with high doping levels, scattering by the ionized dopant atoms becomes an important mechanism that limits mobility. The resistivity versus chlorine vapour pressure is shown in Fig. 1. Independently of the substrate the resistivity of all ZnO:Cl layers decreases with increasing chlorine content in ZnO, showing the effectiveness of chlorine as a shallow donor.

3.2. First principles computations for the band gap of ZnO:Cl

First principles computations were applied in order to examine the change in the band gap of ZnO with Cl doping. We use density functional theory (DFT), in a plane wave basis set [17]. The valence electrons are expanded in a basis of plane waves and the core–valence interaction is treated using the projected augmented wave (PAW) method [18], with an [Ar] core on Zn and a [He] core on O and Cl. The plane wave cut-off is 396 eV and k-space is sampled using Monkhorst–Pack sampling grids. For the smaller supercell (a $2\times2\times2$ expansion), we have used a $(5\times5\times5)$ sampling grid and for the larger supercell (a $(4\times4\times4)$ expansion), we sample at the Γ-point. Fermi level smearing, using the Methfessel–Paxton method, with $\sigma=0.1$ eV is applied. We use the Perdew–Burke–Ernzerhof (PBE) generalised gradient approximation (GGA-DFT)[19]. Since GGA-DFT underestimates the band gap in metal oxides, we apply the DFT+U approach [20], which opens up the band gap. DFT+U has been used in a number of studies on ZnO [21–23], and we set (U–J) to 7.8 eV for the Zn 3d states.

In Fig. 2 we show the structure of wurtzite ZnO doped with Cl. Upon substituting one lattice oxygen with Cl, the smaller supercell gives a Cl concentration of 6.25%. In the larger supercell, substituting one oxygen for Cl gives a Cl concentration of 0.78%, while substituting two oxygen atoms for Cl gives

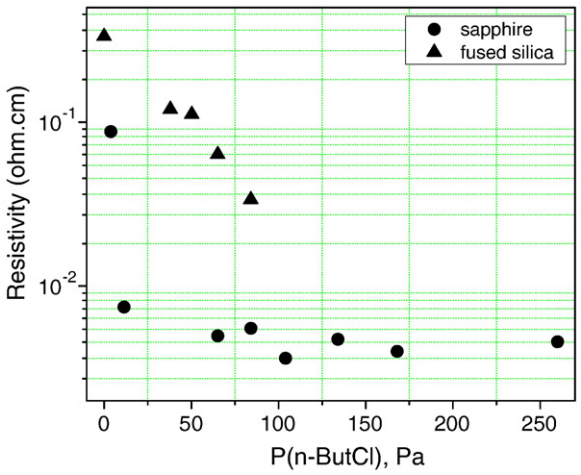

Fig. 1. Room temperature resistivity of ZnO:Cl thin layers deposited on sapphire and fused silica substrates for different vapour pressures of *n*-butyl chloride.

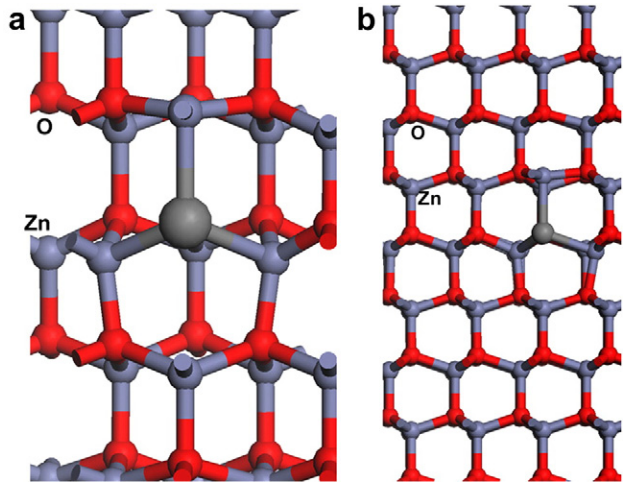

Fig. 2. Supercells of ZnO each with 1 Cl dopant substituting for a lattice oxygen. (a): (2×2×2) supercell, (b): (4×4×4) supercell. Zn and O atoms are indicated in the figure and the dopant is the large grey sphere.

a dopant concentration of 1.56% In the latter, the two Cl atoms are found to be more stable when separated. The ionic positions are fully relaxed (with forces less than 0.02 eV/Å) and all calculations are spin polarised.

Doping of ZnO with up to 6.25% Cl produces a small structural distortion around the dopant site. In stoichiometric ZnO, the Zn–O distances are computed to be 1.97 Å. With 0.78% Cl doping, the Zn–Cl distances range from 2.38–2.43 Å. Similar distortions are found at 6.25% doping. However, these distortions are limited to a small region around the dopant site. They arise simply from the larger ionic radius of the Cl anion (1.81 Å) compared to the oxygen anion (1.40 Å).

To study the impact of Cl doping on the band gap, we have computed the band gap at the Γ-point. For bulk ZnO, the DFT+U computations give a direct band gap of 1.62 eV at the Γ-point, which is improved over GGA-DFT, while still underestimated compared to experiment [24], but consistent with other computations [21–23]. However, changes in band gap by *e.g.* doping are known to be described correctly with DFT. Fig. 3 shows a plot of the change in band gap, ΔE_g, with Cl concentration. We see that there is a small increase in the band gap up to 1.56% Cl doping, which is less than

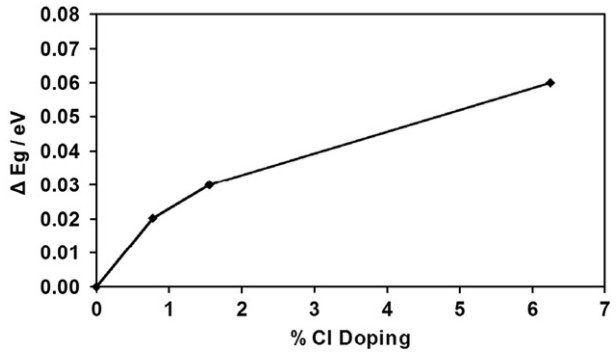

Fig. 3. Computed change in band gap, ΔE_g, as a function of Cl doping concentration for Cl-doped ZnO.

40 meV. At 6.25% Cl doping, the band gap has increased by 60 meV. Fujihara et al. and Hichou et al. found for 5% F-doped ZnO that there was little change in the band gap [25,26], while the results of Sanchez-Juarez et al. [27] indicate that a significantly larger fluorine concentration is needed to increase the band gap. The present results suggest that for Cl doping concentrations around 1%, there will be little change to the band gap, which is consistent with the experimental optical data presented below.

3.3. Optical transmittance

The achievement of a high transparency in the visible to near infra-red (Vis–NIR) spectral range is the second important property, besides high conductivity, for the use of ZnO:Cl films as transparent conductors. The Vis–NIR transmission spectra for ZnO and ZnO:Cl, 0.7 μm thick thin films, deposited on fused silica substrate are presented in Fig. 4. All the results shown were obtained on samples grown with the same amount of DEZ and *t*-but ((P(DEZ)=30 Pa, P(*t*-Bu)=161 Pa). Chlorine vapour pressure was varied from 38 to 86 Pa. For the ZnO:Cl films (curves 1, 2, and 3 in Fig. 4(a)) the transparency in the

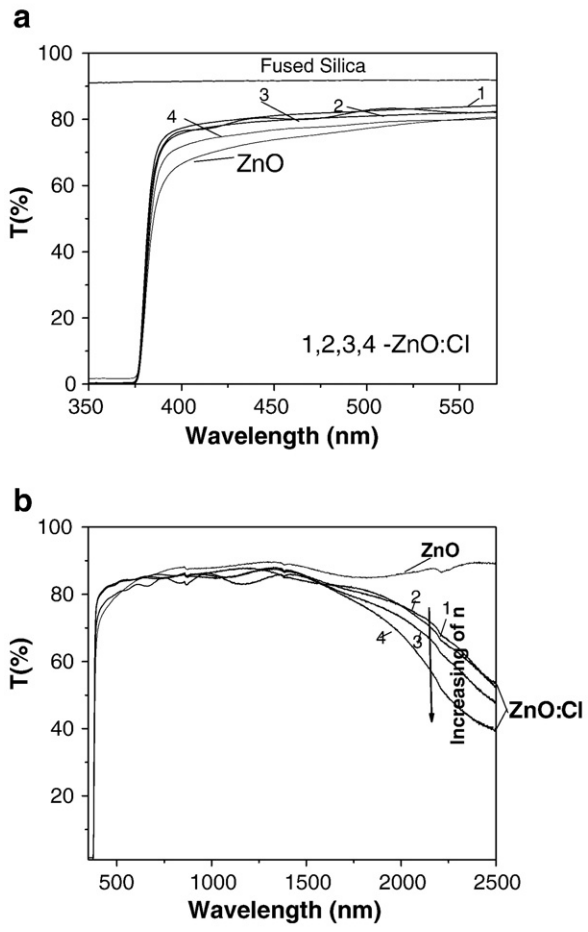

Fig. 4. (a) UV–VIS and (b) NIR optical transmittance for ZnO and ZnO: Cl thin films grown on fused silica. Curve 1, P(*n*-BuCl)=38 Pa; Curve 2, P(*n*-BuCl)=50.3 Pa; Curve 3, P(*n*-BuCl)=65.12 Pa;4–86.27 Pa; for all samples P(DEZ)=30 Pa and P(*t*-Bu)=161 Pa.

visible region is around 80–82%. For the sample with the highest amount of chlorine ($n=1.6\times10^{20}$ cm^{-3}), it decreases to 78–79%, but is still higher than for pure ZnO. This result is probably related to a less scattering surface in the case of ZnO:Cl than for ZnO. Band edge emission does not change with chlorine incorporation. Normally, the variation of band gap with doping, called the Moss effect is observable when the semiconductor is degeneratively doped. Indeed as was shown from computation 1%Cl incorporation can change gap by 40 meV, so in our samples with less than 1% Cl doping, the change in band gap might be small enough that it is not observable in experiment. Transparency of pure ZnO in the 500–1500 nm interval (see Fig. 4(b)) reaches 86% and changes very slightly with doping, while, for $\lambda>1500$ nm, it decreases with increasing the doping level, i.e. with an increasing concentration of free carriers in ZnO:Cl thin films. Though this decrease of transparency is not significant, this means there is no sharp increase of reflectivity in the 1–5 μm region. In other words we do not observe any metallic behavior characteristic of heavily doped TCO [28].

4. Conclusion

In this paper, we have studied the electrical and optical properties of Cl-doped ZnO, which is a potential transparent conducting oxide. Chlorine as an effective donor impurity increases the electron concentration in the layers (up to $\sim10^{20}$ cm^{-3}), resulting in a decrease in the resistivity to $\rho\sim10^{-3}$ Ω cm. Incorporation of less than 1% Cl does not reduce the transparency in the visible region, while a shift in the band gap edge is not observed, meaning that the oxide is not degeneratively doped. Consistent with these first principles computations reveal that a very small band gap change, of less than 40 meV, can be expected with ~1% Cl doping. In summary, we show that at a concentration of less than 1%, chlorine doping of ZnO is effective for increasing the conductivity while retaining the transparency in the visible region required for transparent conducting oxide applications.

Acknowledgments

Work was supported by NATCO-FP6-511925 project. We acknowledge the Science Foundation Ireland/High Education Authority funded Irish Centre for High End Computing for the provision of computational facilities.

References

[1] H.H. Baumach, C. Wagner, Zeits. F. physik. Chemie B 22 (1933) 199.
[2] O. Fritsch, Ann. D. Physik 22 (1935) 375.
[3] A. Guillen-Santiago, M. Olivera, A. Maldonado, et al., Phys. Stat. Sol.(a) 201 (2004) 952.
[4] Byeong-Yun Oh., Min-Chang Jeong, Woong Lee, Jae-Min Myoung, J. Cryst. Growth 274 (2005) 453.
[5] A.V. Singh, M. Kumar, R.M. Mehra, et al., J. Indian Inst. Sci. 81 527 (2001).
[6] Hiroyuki Kato, Michichiro Sano, Kazuhiro Miyamoto, Takafumi Yao, J. Cryst. Growth 273 (2002) 538.
[7] J.D. Ye, S.L. Gu, S.M. Zhu, et al., J. App. Phys. 86 (2005) 192111.
[8] Yasunori Morianga, keijiro Sakuragi, Norufumi Fujilura, Tachiro Ito, J. Cryst. Growth 174 (1997) 691.
[9] F. Paraguay, D.a,c, J. Moralesa, W. Estrada, L.a, E. Andradeb, M. Miki-Yoshid, Thin Solid Films 366 (2000) 16.
[10] L. Castan˜eda, A. Garcı′a-Valenzuel, E.P. Zironi, T, et al., Thin Solid Films 503 (2006) 212.
[11] J. Hu, R.G. Gordon, Sol. Cells 30 (1991) 437.
[12] H.Y. Xu, Y.C. Liu, R. Mu, Appl. Phys. lett. 86 (2005) 123107.
[13] A. Guillen-Santiago, M. Olivera, A. Maldonado, et al., Phys. Stat. Sol. (a) 201 (2004) 952.
[14] B. Hahn, G. Heindel, E. Pschorr-Schoberer, et al., Semic. Sci. Techol. 13 (1998) 788.
[15] Y. Liu, J. Lian, Appl. Surf. Sci. 253 (2007) 3727.
[16] Ellmer, J. Phys. D: Appl. Phys. 34 (2001) 3097.
[17] G. Kresse, J. Furthmüller, Comput. Mater. Sci. 6 (1996) 15;
G. Kresse, J. Furthmüller, Phys. Rev. B 54 (1996) 11169.
[18] P.E. Blöchl, Phys. Rev. B 50 (1994) 17953;
D. Joubert, G. Kresse, Phys. Rev. B 59 (1999) 1758.
[19] J.P. Perdew, K. Burke, M. Ernzerhof, Phys. Rev. Lett. 77 (1996) 3865.
[20] S.L. Dudarev, G.A. Botton, S.Y. Savrasov, C.J. Humphreys, A.P. Sutton, Phys. Rev. B 57 (1998) 1505.
[21] P. Erhart, K. Albe, A. Klein, Phys. Rev. B 73 (2006) 205203.
[22] S. Zh Karazhanov, P. Ravindran, U. Grossner, A. Kjekshus, H. Fjellvag, B.G. Svensson, Solid State Commun. 139 (2006) 391.
[23] R. Laskowski, N.E. Christensen, Phys. Rev. B 73 (2006) 045201.
[24] S.J. Pearton, et al., J. Appl. Phys. 93 (2003) 1.
[25] S. Fujihara, J. Kusakado, T. Kimura, J. Mater. Sci. Lett. 17 (1998) 781.
[26] A. El Hichou, A. Bougrine, J.L. Bubendorff, J. Ebothe, M. Addou, M. Troyon, Semicond. Sci. Technol. 17 (2002) 607.
[27] A. Sanchez-Juarez, A. Tiburcio-Silber, A. Ortiz, E.P. Zironi, J. Rickards, Thin Solid Films 333 (1998) 196.
[28] J. Hamberg, C.G. Granqvist, J. Appl. Phys. 60 (1986) R123.